



**HAL**  
open science

## **Doubling of annual ammonia emissions from the peat fires in Indonesia during the 2015 El Niño**

Simon Whitburn, Martin van Damme, Lieven Clarisse, Solène Turquety,  
Cathy Clerbaux, Pierre-François Coheur

► **To cite this version:**

Simon Whitburn, Martin van Damme, Lieven Clarisse, Solène Turquety, Cathy Clerbaux, et al.. Doubling of annual ammonia emissions from the peat fires in Indonesia during the 2015 El Niño. *Geophysical Research Letters*, 2016, 43 (20), pp.11,007-11,014. 10.1002/2016GL070620 . insu-01375904

**HAL Id: insu-01375904**

**<https://insu.hal.science/insu-01375904>**

Submitted on 3 Aug 2020

**HAL** is a multi-disciplinary open access archive for the deposit and dissemination of scientific research documents, whether they are published or not. The documents may come from teaching and research institutions in France or abroad, or from public or private research centers.

L'archive ouverte pluridisciplinaire **HAL**, est destinée au dépôt et à la diffusion de documents scientifiques de niveau recherche, publiés ou non, émanant des établissements d'enseignement et de recherche français ou étrangers, des laboratoires publics ou privés.



## RESEARCH LETTER

10.1002/2016GL070620

## Key Points:

- NH<sub>3</sub> emissions in Indonesia for 2015 are 2–3 times higher than in the past 7 years
- IASI-derived ammonia emission factors for peatlands are 2.5–8 times lower than those used in GFAS
- First IASI-derived assessment of peat soil combustion

## Supporting Information:

- Supporting Information S1
- Figure S1
- Figure S2

## Correspondence to:

S. Whitburn,  
swhitbur@ulb.ac.be

## Citation:

Whitburn, S., M. Van Damme, L. Clarisse, S. Turquety, C. Clerbaux, and P.-F. Coheur (2016), Doubling of annual ammonia emissions from the peat fires in Indonesia during the 2015 El Niño, *Geophys. Res. Lett.*, 43, 11,007–11,014, doi:10.1002/2016GL070620.

Received 27 JUL 2016

Accepted 27 SEP 2016

Accepted article online 3 OCT 2016

Published online 19 OCT 2016

## Doubling of annual ammonia emissions from the peat fires in Indonesia during the 2015 El Niño

S. Whitburn<sup>1</sup>, M. Van Damme<sup>1</sup>, L. Clarisse<sup>1</sup>, S. Turquety<sup>2</sup>, C. Clerbaux<sup>1,3</sup>, and P.-F. Coheur<sup>1</sup>

<sup>1</sup>Faculté des Sciences, Service de Chimie Quantique et Photophysique, Spectroscopie de l'Atmosphère, Université libre de Bruxelles (U.L.B.), Brussels, Belgium, <sup>2</sup>UMPC University Paris, Ecole Polytechnique, CNRS/INSU, LMD-IPSL, Palaiseau, France, <sup>3</sup>LATMOS/IPSL, UPMC University Paris, Sorbonne Universités, UVSQ, CNRS, Paris, France

**Abstract** In the autumn of 2015, thousands of square kilometers of forest and peatlands in Indonesia went up in flames. Among the primary species emitted by fires, ammonia (NH<sub>3</sub>) is of special relevance for air quality. Here we derive daily and total NH<sub>3</sub> emission fluxes over the affected area using satellite measurements for the years 2008–2015. The 2015 fires emitted an estimated 1.4–8.2 Tg of NH<sub>3</sub> (with a maximum of 0.06–0.33 Tg d<sup>-1</sup>). On an annual basis, the 2015 NH<sub>3</sub> emissions are a factor 2–3 larger than in the previous 7 years. We derive NH<sub>3</sub> emission factors for peat soils, which are found to be 2.5–8 times lower than those used in the GFASv1.2 emission inventory but in excellent agreement with those reported in other recent studies. Finally, we estimate that 3.28 × 10<sup>9</sup> m<sup>3</sup> peat soil was consumed during these 2015 fires, corresponding to an average burn depth of 39 cm.

### 1. Introduction

Indonesia experienced in the autumn of 2015 the most severe forest fires in almost two decades. In the region, fires are generally human induced for land clearing purposes and therefore recurrent [Gaveau *et al.*, 2014]. In 2015, the fires were amplified by the strongest El Niño–Southern Oscillation (ENSO) since 1997, which caused severe droughts throughout the western Pacific [Chisholm *et al.*, 2016]. Fires burned out of control for about 2 months between September and October, mostly on Sumatra and the Indonesian portion of Borneo. They caused the loss of about 2.6 million hectares of tropical forests and peatlands [Glauber *et al.*, 2016], below the 1997–1998 record of 4.56 million hectares [Heil and Goldammer, 2001], and the release of 227 ± 67 Tg of total carbon into the atmosphere [Huijnen *et al.*, 2016]. Peat fires also propagated underground, making them unpredictable and very difficult to control.

The fires greatly impacted the local and regional ecosystems, and atmospheric transport of the fire plumes over the region was responsible for the exposure of 40 million people to hazardous levels of air pollution [Chisholm *et al.*, 2016]. It is anticipated that the fires will have a small but discernible impact on the global climate as was the case in 1997 [Heil and Goldammer, 2001; Page *et al.*, 2002; Harrison *et al.*, 2009]. To assess these impacts, a more accurate determination of the fire emissions is needed. Several estimates have been reported recently for carbon species: Huijnen *et al.* [2016] used the modeling and assimilation framework of the Copernicus Atmosphere Monitoring Service (CAMS) combined with in situ smoke measurements to estimate carbon dioxide (CO<sub>2</sub>), carbon monoxide (CO), and methane (CH<sub>4</sub>) emissions, while Parker *et al.* [2016] derived CH<sub>4</sub> and CO<sub>2</sub> enhancements and biomass burning emission ratios from the measurements of the Greenhouse gases Observing SATellite (GOSAT). More recently, Stockwell *et al.* [2016] calculated emission factors (EFs) for peatlands from in situ measurements for a series of trace gases. No studies on total emissions have been conducted up to now for noncarbon species such as NH<sub>3</sub>, which is of prime importance to the environment since it is known to be responsible for eutrophication and acidification of the ecosystems. In the atmosphere, it combines with acid gases (mostly sulfuric acid (H<sub>2</sub>SO<sub>4</sub>), nitric acid (HNO<sub>3</sub>), and hydrochloric acid (HCl)) resulting in the formation of secondary aerosols that in turn impact climate and human health.

In this paper, we determine and analyze the atmospheric ammonia (NH<sub>3</sub>) emissions from the 2015 Indonesian fires based on satellite observations and we derive new EF<sub>NH<sub>3</sub></sub> from peatlands for this event. The use of satellite observations offers the possibility to follow a particular event throughout its entire duration and spatial extent owing to the good spatial and temporal coverage compared to airborne and ground-based measurements. This is particularly true for the Infrared Atmospheric Sounding Interferometer (IASI) instrument used here,

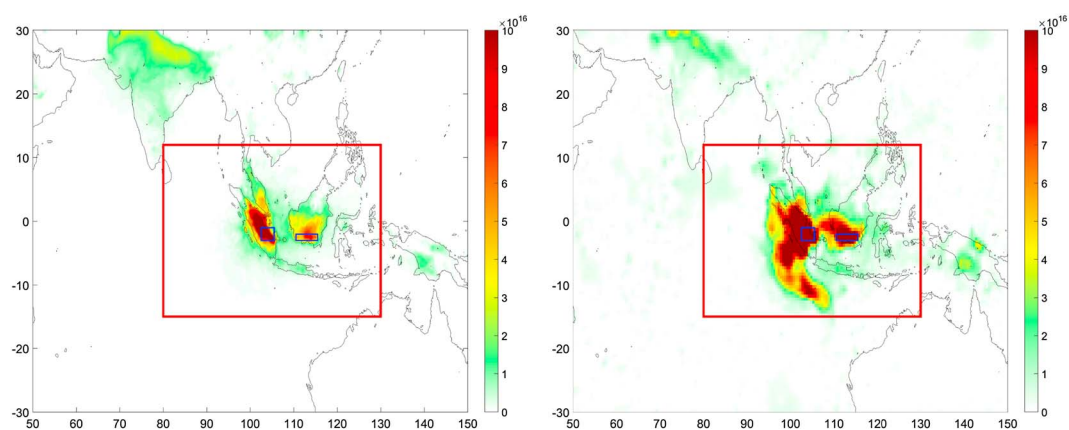


**Figure 1.** (left)  $\text{NH}_3$  total columns ( $\text{molec cm}^{-2}$ ) from IASI measurements (morning overpasses) between August and November 2015 on a  $0.5^\circ$  by  $0.5^\circ$  grid. The distribution is an arithmetic mean of all measurements within a cell. The red rectangle shows the studied area for fluxes calculation. The blue rectangles show the studied areas for the calculation of the  $\text{NH}_3$  enhancement ratios relative to CO. (right)  $\text{NH}_3$  total columns ( $\text{molec cm}^{-2}$ ) measured on a single day, 25 October 2015, (MetOp A and B) distributed on a  $0.5^\circ$  by  $0.5^\circ$  grid.

which has exceptional sampling. We discuss these emissions in a multiple-year perspective using available measurements since 2008. The quantification of  $\text{NH}_3$  emissions from fires is important to assess, on one hand, how much of the nitrogen pool in the soil was consumed and, on the other hand, the contribution of the nitrogen species on the degradation of air quality and ecosystem health. We also derive a first top-down estimation of the amount of peat soils that was consumed during the event.

## 2. IASI Satellite Measurements of $\text{NH}_3$ and CO

The 2015 fires in Indonesia provide an excellent case for the study of  $\text{NH}_3$  wildfire emissions from satellite since (1) forests and peatlands burned with a high intensity during a long time period, (2) fires were restricted to a limited area, and (3) they occurred far away from other sources of  $\text{NH}_3$ . Most of the results in this paper are obtained using the measurements from the Infrared Atmospheric Sounding Interferometer (IASI), a hyper-spectral infrared sounder on board the polar Sun-synchronous MetOp satellites. It covers the entire globe twice daily (crossing the equator at 9:30 and 21:30 local solar time) with a relatively small footprint on the ground (circular pixel of 12 km diameter at nadir), a good spectral resolution ( $0.5 \text{ cm}^{-1}$  apodized) [Clerbaux *et al.*, 2009] and a dense spatial coverage (compared to other similar instruments, such as TES) [Shephard *et al.*, 2011]. Only daytime measurements were used in this work because of the generally more favorable thermal contrast prevailing during daytime in the region compared to nighttime. The retrieval of  $\text{NH}_3$  is based on a new robust and flexible algorithm [Whitburn *et al.*, 2016]. We also used in support to our analysis CO tropospheric columns retrieved from IASI using the FORLI algorithm [Hurtmans *et al.*, 2012]. The FORLI-CO columns have been intercompared and validated [George *et al.*, 2015] and used in several previous studies in relation to fire emission and transport [e.g., Krol *et al.*, 2013].

The exceptional character of the 2015 fires is shown in Figure 1. Figure 1 (left) shows the mean  $\text{NH}_3$  total columns ( $\text{molec cm}^{-2}$ ) distribution (MetOp A and B measurements) between August and November 2015 in a  $0.5^\circ$  by  $0.5^\circ$  grid. Figure 1 (right) shows the (transported)  $\text{NH}_3$  fire plume ( $\text{molec cm}^{-2}$ ) and emission sources measured on 25 October 2015. Here and elsewhere in this study, only total columns with a relative error lower than 100% or an absolute error lower than  $7.5 \times 10^{15} \text{ molec cm}^{-2}$  and a cloud contamination lower than 25% are retained. Doing this, low columns typical for background conditions with a large relative error but a small absolute error are also taken into account, reducing the high bias reported in other studies [Van Damme *et al.*, 2014]. High  $\text{NH}_3$  total columns are found above Indonesia, mostly in the eastern part of Sumatra and in the Indonesian portion of Borneo in agreement with the localization of the fire hot spots. The highest mean columns reach  $1.6 \times 10^{17} \text{ molec cm}^{-2}$  which is 3–4 times larger than those over India that usually dominate the distribution in the same time period. Transported plumes over the Indian Ocean are also clearly visible, especially on the daily  $\text{NH}_3$  total column ( $\text{molec cm}^{-2}$ ) distributions (Figure 1, right).

When quantifying trace gas emissions from fires, an important parameter is the emission factor ( $\text{EF}_x$ ), which is defined as the mass of a trace gas X emitted per kilogram of biomass burned ( $\text{g kg}^{-1}$  dry matter (DM)). As it

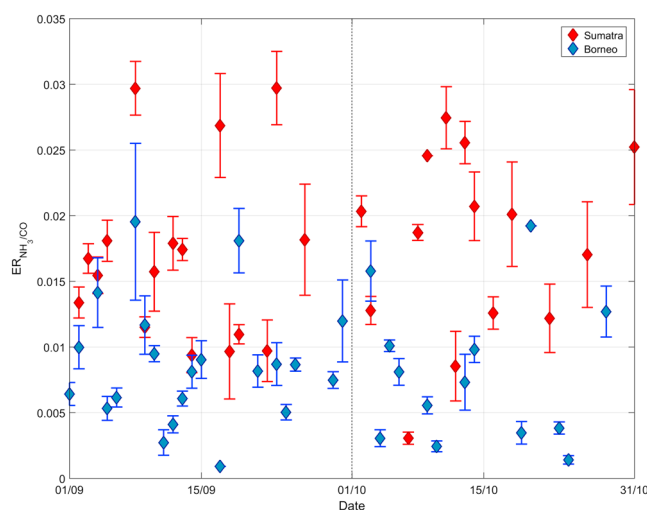


**Figure 2.** Daily  $\text{NH}_3$  enhancement ratios relative to CO ( $\text{ER}_{\text{NH}_3/\text{CO}}$ ) calculated from the slope of the linear regression of  $\text{NH}_3$  versus CO total columns between 1 September and 31 October 2015, over Sumatra (red) and Borneo (blue). The error bars correspond to the standard errors on the regression slope. Daily  $\text{ER}_{\text{NH}_3/\text{CO}}$  with a correlation coefficient  $< 0.3$  for the slope have been excluded.

cannot be derived from satellite measurements directly, a related parameter, the enhancement ratios (ERs), is frequently used. The  $\text{ER}_{\text{NH}_3/\text{CO}}$  is defined as the ratio of the number of emitted molecules of  $\text{NH}_3$  (or the  $\text{NH}_3$  total column) over the emitted molecules of CO (or the CO total column, the reference species) [Goode *et al.*, 2000; R'Honi *et al.*, 2013]:

$$\text{ER}_{\text{NH}_3/\text{CO}} = \frac{[\text{NH}_3]_{\text{smoke}} - [\text{NH}_3]_{\text{ambient}}}{[\text{CO}]_{\text{smoke}} - [\text{CO}]_{\text{ambient}}} \quad (1)$$

As enough measurements are available from IASI, daily average ERs can best be estimated from the slope of the linear regression of  $\text{NH}_3$  versus CO total columns (by considering each IASI measurement) [Andreae and Merlet, 2001; Coheur *et al.*, 2009]. We have calculated the daily mean  $\text{ER}_{\text{NH}_3/\text{CO}}$  separately over the two principal burning areas in the region (blue rectangles in Figure 1) between 1 September and 31 October 2015. The first is in Sumatra and extends from  $3-1^\circ \text{ S}$  to  $102.5-105.5^\circ \text{ E}$  and the other is in the Indonesian portion of Borneo from  $3-2^\circ \text{ S}$  to  $110.5-115.5^\circ \text{ E}$ . The 2 months time series of the daily mean  $\text{ER}_{\text{NH}_3/\text{CO}}$  ( $\pm$  standard error) is shown in Figure 2. Note that the  $\text{ER}_{\text{NH}_3/\text{CO}}$  with a correlation coefficient of the linear regression (between  $\text{NH}_3$  and CO) lower than 0.3 were excluded from the analysis. While we do not find a clear trend in the evolution of the  $\text{ER}_{\text{NH}_3/\text{CO}}$  during the 2 months, there are significant differences between the two areas, with  $\text{ER}_{\text{NH}_3/\text{CO}}$  almost systematically higher for Sumatra ( $17.3 \times 10^{-3} \pm 6.8 \times 10^{-3}$ , on average) than for Borneo ( $8.4 \times 10^{-3} \pm 4.9 \times 10^{-3}$ ). Since peat soils were found to be the dominant contribution to the emissions during the fire event (especially for reduced species) [Huijnen *et al.*, 2016], the measured  $\text{ER}_{\text{NH}_3/\text{CO}}$  can be considered representative of the  $\text{ER}_{\text{NH}_3/\text{CO}}$  for peatlands. In this regard, observed differences in  $\text{ER}_{\text{NH}_3/\text{CO}}$  between the two regions are in agreement with the measurements of Stockwell *et al.* [2014] who found much higher  $\text{EF}_{\text{NH}_3}$  for peat soils in Sumatra than in Borneo, despite the similarities in the percent nitrogen content.

### 3. Fluxes, Masses and Emission Factors

#### 3.1. $\text{NH}_3$ Flux Emissions and Masses

IASI total columns of  $\text{NH}_3$  ( $\text{molec.cm}^{-2}$ ) were converted to daily fluxes ( $\text{Tg NH}_3 \text{ d}^{-1}$ ) using a simplified box model similar to R'Honi *et al.* [2013] and Whitburn *et al.* [2015] and considering four different effective lifetimes ( $\tau_{\text{eff}}$ ) for  $\text{NH}_3$  of 6 h, 12 h, 24 h and 36 h (since the effective lifetime of  $\text{NH}_3$  is unknown and highly variable) in agreement with the  $\text{NH}_3$  lifetime reported in Dentener and Crutzen [1994]; Aneja *et al.* [2001] and R'Honi *et al.* [2013]. Details of the methodology are given in Text S1 in the supporting information. The domain considered for the calculation, extending from  $15^\circ \text{ S}$  to  $12^\circ \text{ N}$  in latitude and from  $80^\circ$  to  $130^\circ \text{ E}$  in longitude (red rectangle in Figure 1), was selected to include the majority of the transported  $\text{NH}_3$  plumes. Note that this selected region does not show other significant sources of emissions.

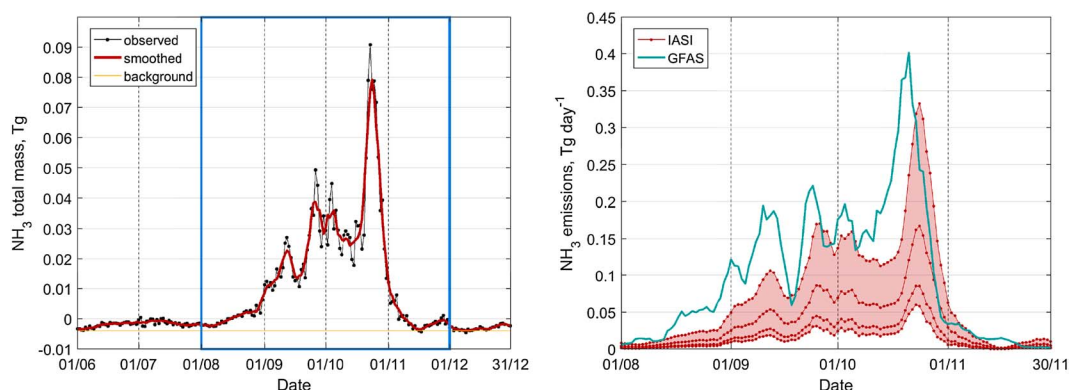


**Figure 3.** (left) Daily total  $\text{NH}_3$  masses in Tg (black dots and red line) over the area  $15^\circ \text{S} - 12^\circ \text{N}$ ,  $80 - 130^\circ \text{E}$  between June and December 2015. The red line represents the 5 day simple moving average total masses; the yellow line corresponds to the background total masses used for the calculation of the daily fluxes. (right)  $\text{NH}_3$  emission fluxes in  $\text{Tg d}^{-1}$  between August and November 2015 (period defined by the blue rectangle on Figure 3, left) using four different effective lifetimes for  $\text{NH}_3$ : 6, 12, 24, and 36 h. The shaded area corresponds to the set of possible values of  $\text{NH}_3$  emission fluxes within the range of values given by the different effective lifetimes (red lines). The cyan line correspond to the 5 day moving average  $\text{NH}_3$  emissions from the GFASv1.2 inventory.

Figure 3 (left panel) shows for the period extending from June 1 to December 31 the daily total masses in Tg (in black daily values and in red 5 day simple moving average) above the studied area. We find large daily amounts of  $\text{NH}_3$  between September 10 and the end of October with daily total masses between 0.02 and 0.04 Tg  $\text{NH}_3$  and a peak value at 0.08 Tg around 20–25 October. For the sake of comparison, these peak emitted masses are about 1.5–2 times larger than the daily total masses reported in *R'Honi et al.* [2013] for the 2010 Russian fires, for a surface which is about 40% smaller. These observed differences can be explained by differences in the type of burned fuel, since both peatlands and boreal forest were affected during the 2010 Russian fires. After October 31, mean  $\text{NH}_3$  columns (Figure 1) and total masses (Figure 3) quickly return to background values because of the short lifetime of  $\text{NH}_3$  and the end of fires associated with the arrival of rain.

The right panel in Figure 3 shows the  $\text{NH}_3$  emission fluxes ( $\text{Tg d}^{-1}$ ) between August 1 and November 30, with a mean background value subtracted. The latter is taken as the minimum of the total masses observed in 6 months intervals and is represented by a yellow line on the left panel. Note that this subtraction process leads to a slight overestimation in background conditions as the total emitted masses can be negative (Figure 3, left panel). As mentioned above,  $\text{NH}_3$  emission fluxes are calculated by considering four different effective lifetimes for  $\text{NH}_3$  (6 h, 12 h, 24 h and 36 h) and the results are presented as a set of possible values of  $\text{NH}_3$  fluxes (shaded area) within the range of values given by the different lifetimes (red lines). The maximum  $\text{NH}_3$  flux is calculated for October 24 with values between 0.06 and 0.33  $\text{Tg d}^{-1}$ . Higher values are expected for the smaller effective lifetime. By summing the daily emission fluxes over the whole period (between 1 September and 31 October), the total emissions for the event are calculated to be, respectively, 1.4, 2.1, 4.1, and 8.2 Tg and make up 76% of the total emissions for the year 2015 within the studied region.

### 3.2. Comparison With the GFAS Inventory and Calculation of New EF

These calculated fluxes from IASI measurements can be compared with these from the Global Fire Assimilation System (GFASv1.2) biomass burning emission inventory (cyan line on Figure 3) which rely for the estimation of the emissions fluxes on the linear relationship between the biomass burned in a fire and the radiative energy it releases [*Kaiser et al.*, 2012]. We find systematically higher fluxes for the bottom-up (GFAS) than for the top-down (IASI) estimates, even when considering an effective lifetime of 6 h for  $\text{NH}_3$ . These observed differences could point to underestimation of the IASI  $\text{NH}_3$  columns, but it is unlikely that this is the main factor responsible as large  $\text{NH}_3$  columns lead to larger spectral signatures and reduced measurement uncertainties. It is also possible that the assumed  $\text{NH}_3$  lifetime is still too large, leading to an underestimation of the calculated daily fluxes. To examine this possibility, we have estimated a mean effective lifetime of  $\text{NH}_3$  from the IASI measurements on multiple days (seven) showing a well-marked transported plume (see Text S2, Table S1, and Figure S1 in the supporting information). We find a mean lifetime of about 21 h which is well in the range used to calculate the emission fluxes. Finally, it is possible that the emissions are overestimated in GFAS through an overestimation of the  $\text{EF}_{\text{NH}_3}$ .

**Table 1.**  $EF_{NH_3}$  in  $g\ kg^{-1}$  Dry Matter Derived From the Total  $NH_3$  Emissions ( $E_{NH_3}(tot)$ ) for Different Effective Lifetimes ( $\tau_{eff}$ ) for  $NH_3$ 

$\tau_{eff}$ (h)	12	21	24	30	36
$E_{NH_3}(tot)$ (Tg)	4.1	2.3	2.1	1.7	1.4
$EF_{NH_3}$ ( $g\ kg^{-1}$ DM)	7.7	4.2	3.7	2.9	2.4

<sup>a</sup>The 21 h lifetime corresponds to that determined empirically (see Text S2 in the supporting information).

To explore this last possibility, we focus on the fraction of emissions related to peat soils which dominated, by far, the total emissions [Huijnen *et al.*, 2016]. In support to this analysis, we use CO emissions estimated from the IASI CO total columns following the same method as for  $NH_3$  (see section 3.1) and for which the EFs used in the emission inventories are thought to be more reliable. Note that a larger domain than for  $NH_3$  was considered ( $30^\circ S - 30^\circ N$  and  $40 - 150^\circ E$ ) because of the longer lifetime of CO (of about a week to months [Holloway *et al.*, 2000; Yurganov *et al.*, 2011]). The comparison of the IASI-derived daily CO emissions fluxes (calculated for three different lifetimes: 7, 15, and 30 days) with GFAS (see Figure S2) gives a good correspondence, especially when considering a lifetime of 30 days for CO, with differences of 13% on average. Over the whole fire period (between 1 September and 31 October), we find total emissions of CO of about 122 Tg. Based on the results of Huijnen *et al.* [2016], we consider that about 90% of these (i.e., 110 Tg) are attributed to CO originating from burning peatland. The remaining 12 Tg are attributed to tropical forests. Assuming that the other EFs used in GFAS are valid, we can then derive an average  $EF_{NH_3}$  for peatlands for this specific event following

$$E_{CO}(peat) \times \frac{EF_{NH_3}(peat)}{EF_{CO}} + E_{CO}(TF) \times \frac{EF_{NH_3}(TF)}{EF_{CO}} = E_{NH_3}(tot) \quad (2)$$

with  $E_{CO}(peat)$  (= 110 Tg) and  $E_{CO}(TF)$  (= 12 Tg) the fraction of CO emissions originating from peatlands and tropical forests, and  $E_{NH_3}(tot)$  the total  $NH_3$  emissions calculated by considering different effective lifetime for  $NH_3$  (between 12 h and 36 h; see Table 1);  $EF_{CO}(peat) = 210\ g\ kg^{-1}\ DM$ ,  $EF_{CO}(TF) = 101\ g\ kg^{-1}\ DM$ ,  $EF_{NH_3}(TF) = 0.93\ g\ kg^{-1}\ DM$ . We find this way an  $EF_{NH_3}$  for peatland between 2.4 (for the 36 h lifetime) and 7.7 (12 h lifetime)  $g\ kg^{-1}\ DM$ . It is, as expected, lower than the one used in GFAS (=  $20\ g\ kg^{-1}\ DM$ ), by a factor 2.5–8 and than the one given in Akagi *et al.* [2011] ( $10.8\ g\ kg^{-1}\ DM$ , derived from Indonesian and boreal peat), but is in excellent agreement with the EFs reported by Stockwell *et al.* [2014] specifically for Indonesian peat ( $7.57\ g\ kg^{-1}\ DM$ ) using open-path Fourier transform infrared spectroscopy. More recently, Stockwell *et al.* [2016] measured even lower  $EF_{NH_3}$  for the peat soils ( $2.86 \pm 1.00\ g\ kg^{-1}\ DM$ ) for the 2015 fires, but their analyses were restricted to the Borneo island. Including our new estimate of  $EF_{NH_3}(peat)$  in equation (2), we conclude that 90–98% of the  $NH_3$  emitted in 2015 originated from peatlands.

A second estimate of  $NH_3$  emission factors,  $EF_{NH_3}^*$ , can be derived from  $ER_{NH_3/CO}$  (estimated in section 2). Since they were measured in the immediate vicinity of the emission sources, the two quantities are related via

$$EF_{NH_3}^* = ER_{NH_3/CO} \times \frac{MM_{NH_3}}{MM_{CO}} \times EF_{CO}, \quad (3)$$

where  $MM_{NH_3}$  and  $MM_{CO}$  are the molar masses of  $NH_3$  and CO, and  $EF_{CO}$  is taken as the one used in GFAS for peatlands (=  $210\ g\ kg^{-1}\ DM$ ). This gives  $EF_{NH_3}^*$  of  $2.21 (\pm 0.86)$  and  $1.07 (\pm 0.63)\ g\ kg^{-1}\ DM$  for Sumatra and Borneo, respectively, which is in good agreement with the  $EF_{NH_3}$  derived from equation (2) when considering the effective lifetime of 36 h for  $NH_3$  (=  $2.4\ g\ kg^{-1}\ DM$ ). The  $EF_{NH_3}^*$  should be taken as a lower bound since (1) they also include the emissions from nonpeat fires with lower specific  $EF_{NH_3}$  and (2) they do not take into account the accumulation of CO in the area.

Given the above, we conclude that the average  $EF_{NH_3}$  for the Indonesian peatlands is probably in between  $EF_{NH_3}^*$  and  $EF_{NH_3}$  estimated with the lower lifetime of 12 h for  $NH_3$ , i.e., between  $2.21\ g\ kg^{-1}\ DM$  and  $7.7\ g\ kg^{-1}\ DM$ . This is much lower than the factor applied to peatland emissions in GFAS and likely explains the high flux values in the inventory.

### 3.3. Comparison With the Previous Years and Estimation of Burned Peat Soils

The exceptional character of the 2015 emissions in the perspective of the previous years is illustrated in Figure 4 where the daily fluxes ( $Tg\ d^{-1}$ ) calculated over the period 2008–2015 considering the IASI-derived

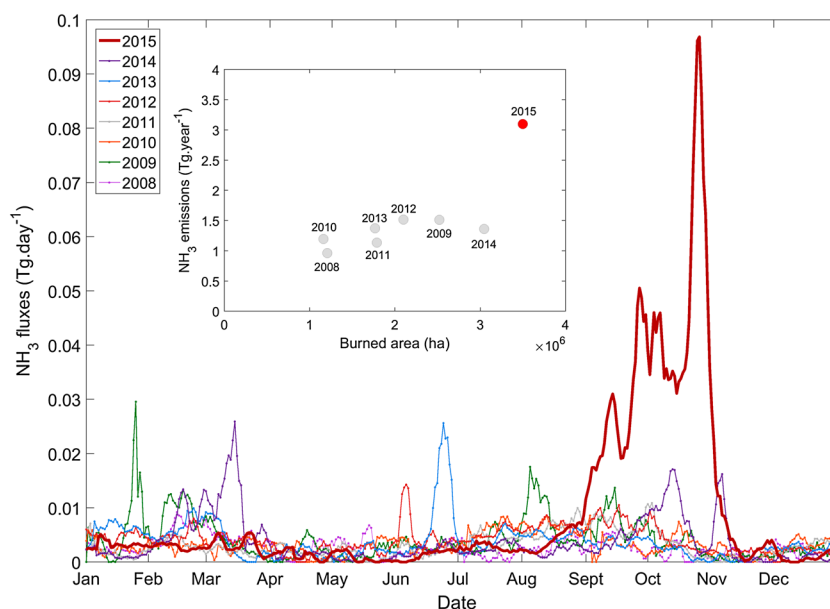


**Figure 4.** NH<sub>3</sub> emission fluxes in Tg d<sup>-1</sup> (5 day simple moving average) between 2008 and 2015 by considering the empirically derived effective lifetime of 17 h for NH<sub>3</sub>. (inset) Cumulated annual NH<sub>3</sub> emissions fluxes in Tg yr<sup>-1</sup> calculated from the daily NH<sub>3</sub> emissions fluxes (Tg d<sup>-1</sup>) (considering the same effective lifetime of 17 h for NH<sub>3</sub>) relative to the total annual burned area (ha) for the region (15° S–12° N, 80–130° E).

lifetime of 21 h for NH<sub>3</sub> are shown, as well as the yearly fluxes (Tg yr<sup>-1</sup>) relative to the Global Fire Emissions Database Version 4 (GFEDv4) burned area (ha) [Randerson *et al.*, 2015] for the same period (inset). On a daily basis (Figure 4), we find that emission fluxes at the peak in 2015 are 3 to 6 times higher than for the seven previous years, which have maximum generally between 0.015 and 0.03 Tg d<sup>-1</sup>. Note also the presence of marked peaks of NH<sub>3</sub> emissions (although much weaker than the peak of autumn 2015) for the relative large fires of June 2013 [Gaveau *et al.*, 2014] and for the period between February and March 2014. On a yearly basis (Figure 4, inset), we find that the annual NH<sub>3</sub> emissions for the year 2015 (3.1 Tg yr<sup>-1</sup>) are as well 2–3 times higher than the annual emissions for the period 2008–2014, but interestingly, this is not systematically the case of the burned area. This is especially true for the years 2009 and 2014 for which we calculate annual NH<sub>3</sub> emissions about 2 times lower than for the year 2015 while the corresponding burned areas are only 13–29% lower. We interpret this as differences in the fraction of peatland burned compared to tropical forest (since peatlands and tropical forests have very different EF<sub>NH<sub>3</sub></sub>) but also in the burn depth of the peat soils, which is known to be highly variable from one fire event to another [van der Werf *et al.*, 2010]. Based on the GFEDv4 burned area [Randerson *et al.*, 2015], we find that close to  $8.5 \times 10^5$  ha peatland burned during the 2 months period of the fires. Following the same methodology as in Huijnen *et al.* [2016] but using the IASI data (details of the procedure are given in Text S3 in the supporting information), we estimate a total loss of  $3.28 \times 10^9$  m<sup>3</sup> of peat soils for the fire event of 2015 (considering a peat bulk density of 0.16 g cm<sup>3</sup>), which translates to an average loss of 62 kg DM m<sup>-2</sup> and an average burn depth of 39 cm. This is about 13 cm deeper than what was calculated by Huijnen *et al.* [2016] based on CO<sub>2</sub> emissions from bottom-up approaches but well in the range of burn depths (18–60 cm) measured by Stockwell *et al.* [2016] at different sites in Borneo. It is important to keep in mind that the derived amount of burned peat soil is directly proportional to the chosen lifetime for CO in the calculation of the emissions (here 30 days) which remains uncertain and variable. Nevertheless, it should be emphasized that it is the first time we are able to estimate how much peat soils were consumed during a fire event (and to what depth) using a top-down approach.

#### 4. Conclusion

In this work, we have given a first top-down estimation of how much NH<sub>3</sub> was emitted during the 2015 Indonesia's peat and forest fires using IASI observations combined to a simple box model with first-order loss in NH<sub>3</sub>. We found maximum daily emissions of about 3 to 6 times higher than the emissions from the seven previous years (2008–2014). From the NH<sub>3</sub> (and CO) emissions, we derived new EF<sub>NH<sub>3</sub></sub> for peatlands in the range

2.4–7.7 g kg<sup>-1</sup> dry matter (DM), depending on the lifetime considered for NH<sub>3</sub> (between 12 and 36h). These values suggest an overestimation of the EF<sub>NH<sub>3</sub></sub> used in GFAS and given in Akagi *et al.* [2011] by a factor 4 to 8. The new EF<sub>NH<sub>3</sub></sub> were also supported by the low EF<sub>NH<sub>3</sub></sub><sup>\*</sup> (at around 1–2 g kg<sup>-1</sup> DM) derived from the NH<sub>3</sub> enhancement ratios relative to CO (ER<sub>NH<sub>3</sub>/CO</sub>) over the two principal fire source areas (Sumatra and Borneo). Finally, we have also provided a top-down assessment of how much peat soils was consumed, following the same methodology as in Huijnen *et al.* [2016]. We found a total loss of 3.28 × 10<sup>9</sup> m<sup>3</sup> of peatlands, corresponding to an average burn depth of 39 cm, in good agreement with Huijnen *et al.* [2016] and Stockwell *et al.* [2016].

#### Acknowledgments

We thank the reviewers very much for their positive feedback on the paper and their useful comments. The NH<sub>3</sub> IASI data used in this work are freely available for all users through the the Aeris data infrastructure (<http://www.aeris-data.fr>; Aeris, 2016). We acknowledge the use of the emission inventory GFASv1.2 and the GFEDv4 burned area data. Data from the emission inventory GFASv1.2 are available on <http://www.gmes-atmosphere.eu>. GFEDv4 burned area data are available on <http://www.globalfiredata.org/>. IASI has been developed and built under the responsibility of the Centre National d'Études Spatiales (CNES, France). It is flown on board the MetOp satellites as part of the EUMETSAT Polar System. The IASI L1 data are received through the EUMETCast near real-time data distribution service. The research in Belgium was funded by the F.R.S.-FNRS and the Belgian State Federal Office for Scientific, Technical and Cultural Affairs (Prodex arrangement IASI.FLOW). S. Whitburn is grateful for his Ph.D. grant (Boursier FRIA) to the "Fonds pour la Formation à la Recherche dans l'Industrie et dans l'Agriculture" of Belgium. L. Clarisse is Research Associate (Chercheur Qualifié) with the Belgian F.R.S.-FNRS. C. Clerbaux and S. Turquety are grateful to CNES for scientific collaboration and financial support.

#### References

- Akagi, S. K., R. J. Yokelson, C. Wiedinmyer, M. J. Alvarado, J. S. Reid, T. Karl, J. D. Crouse, and P. O. Wennberg (2011), Emission factors for open and domestic biomass burning for use in atmospheric models, *Atmos. Chem. Phys.*, *11*(9), 4039–4072, doi:10.5194/acp-11-4039-2011.
- Andreae, M., and P. Merlet (2001), Emission of trace gases and aerosols from biomass burning, *Global Biogeochem. Cycles*, *15*(4), 955–966.
- Aneja, V. P., B. Bunton, J. T. Walker, and B. P. Malik (2001), Measurement and analysis of atmospheric ammonia emissions from anaerobic lagoons, *Atmos. Environ.*, *35*(11), 1949–1958.
- Chisholm, R. A., L. S. Wijedasa, and T. Swinfield (2016), The need for long-term remedies for Indonesia's forest fires: Letter, *Conserv. Biol.*, *30*(1), 5–6, doi:10.1111/cobi.12662.
- Clerbaux, C., et al. (2009), Monitoring of atmospheric composition using the thermal infrared IASI/MetOp sounder, *Atmos. Chem. Phys.*, *9*, 6041–6054, doi:10.5194/acp-9-6041-2009.
- Coheur, P.-F., L. Clarisse, S. Turquety, D. Hurtmans, and C. Clerbaux (2009), IASI measurements of reactive trace species in biomass burning plumes, *Atmos. Chem. Phys.*, *9*, 5655–5667, doi:10.5194/acp-9-5655-2009.
- Dentener, F., and P. Crutzen (1994), A three-dimensional model of the global ammonia cycle, *J. Atmos. Chem.*, *19*, 331–369.
- Gaveau, D. L. A., et al. (2014), Major atmospheric emissions from peat fires in Southeast Asia during non-drought years: Evidence from the 2013 Sumatran fires, *Sci. Rep.*, *4*, 6112, doi:10.1038/srep06112.
- George, M., et al. (2015), An examination of the long-term CO records from MOPITT and IASI: Comparison of retrieval methodology, *Atmos. Meas. Tech.*, *8*(10), 4313–4328, doi:10.5194/amt-8-4313-2015.
- Glauber, A. J., S. Moyer, M. Adriani, and I. Gunawan (2016), *The Cost of Fire: An Economic Analysis of Indonesia's 2015 Fire Crisis*, Indonesia Sustainable Landscapes Knowledge, Note No. 1, World Bank, Jakarta.
- Goode, J. G., R. J. Yokelson, D. E. Ward, R. A. Susott, R. E. Babbitt, M. A. Davies, and W. M. Hao (2000), Measurement of excess O<sub>3</sub>, CO<sub>2</sub>, CO, CH<sub>4</sub>, C<sub>2</sub>H<sub>4</sub>, C<sub>2</sub>H<sub>2</sub>, HCN, NO, NH<sub>3</sub>, HCOOH, CH<sub>3</sub>COOH, HCHO, and CH<sub>3</sub>OH in 1997 Alaskan biomass burning plumes by airborne Fourier transform infrared spectroscopy (AFTIR), *J. Geophys. Res.*, *105*(D17), 147–166.
- Harrison, M. E., S. E. Page, and S. H. Limin (2009), The global impact of Indonesian forest fires, *Biologist*, *56*(3), 156–163.
- Heil, A., and J. G. Goldammer (2001), Smoke-haze pollution: A review of the 1997 episode in Southeast Asia, *Reg. Environ. Change*, *2*(1), 24–37, doi:10.1007/s101130100021.
- Holloway, T., H. Levy, and P. Kasibhatla (2000), Global distribution of carbon monoxide, *J. Geophys. Res.*, *105*(D10), 12,123–12,147, doi:10.1029/1999JD901173.
- Huijnen, V., M. J. Wooster, J. W. Kaiser, D. L. A. Gaveau, J. Flemming, M. Parrington, A. Inness, D. Murdiyarso, B. Main, and M. van Weele (2016), Fire carbon emissions over maritime southeast Asia in 2015 largest since 1997, *Sci. Rep.*, *6*, 26886, doi:10.1038/srep26886.
- Hurtmans, D., P.-F. Coheur, C. Wespes, L. Clarisse, O. Scharf, C. Clerbaux, J. Hadji-Lazaro, M. George, and S. Turquety (2012), FORLI radiative transfer and retrieval code for IASI, *J. Quant. Spectrosc. Radiat. Transfer*, *113*(11), 1391–1408, doi:10.1016/j.jqsrt.2012.02.036.
- Kaiser, J. W., et al. (2012), Biomass burning emissions estimated with a global fire assimilation system based on observed fire radiative power, *Biogeosciences*, *9*(1), 527–554, doi:10.5194/bg-9-527-2012.
- Krol, M., et al. (2013), How much CO was emitted by the 2010 fires around Moscow?, *Atmos. Chem. Phys.*, *13*(9), 4737–4747, doi:10.5194/acp-13-4737-2013.
- Page, S., F. Siebert, J. Rieley, H.-D. V. Boehm, A. Jaya, and S. Limin (2002), The amount of carbon released from peat and forest fires in Indonesia during 1997, *Nature*, *420*, 61–65, doi:10.1038/nature01131.
- Parker, R. J., H. Boesch, M. J. Wooster, D. P. Moore, A. J. Webb, D. Gaveau, and D. Murdiyarso (2016), Atmospheric CH<sub>4</sub> and CO<sub>2</sub> enhancements and biomass burning emission ratios derived from satellite observations of the 2015 Indonesian fire plumes, *Atmos. Chem. Phys.*, *16*(15), 10,111–10,131, doi:10.5194/acp-16-10111-2016.
- Randerson, J. T., G. van der Werf, L. Giglio, G. J. Collatz, and P. Kasibhatla (2015), *Global Fire Emissions Database, Version 4 (GFEDv4)*, ORNL DAAC, Oak Ridge, Tennessee.
- R'Honi, Y., L. Clarisse, C. Clerbaux, D. Hurtmans, V. Duflet, S. Turquety, Y. Ngadi, and P.-F. Coheur (2013), Exceptional emissions of NH<sub>3</sub> and HCOOH in the 2010 Russian wildfires, *Atmos. Chem. Phys.*, *13*(8), 4171–4181, doi:10.5194/acp-13-4171-2013.
- Shepard, M. W., et al. (2011), TES ammonia retrieval strategy and global observations of the spatial and seasonal variability of ammonia, *Atmos. Chem. Phys.*, *11*(20), 10,743–10,763, doi:10.5194/acp-11-10743-2011.
- Stockwell, C. E., R. J. Yokelson, S. M. Kreidenweis, A. L. Robinson, P. J. DeMott, R. C. Sullivan, J. Reardon, K. C. Ryan, D. W. T. Griffith, and L. Stevens (2014), Trace gas emissions from combustion of peat, crop residue, domestic biofuels, grasses, and other fuels: configuration and Fourier transform infrared (FTIR) component of the fourth Fire Lab at Missoula Experiment (FLAME-4), *Atmos. Chem. Phys.*, *14*(18), 9727–9754, doi:10.5194/acp-14-9727-2014.
- Stockwell, C. E., et al. (2016), Field measurements of trace gases and aerosols emitted by peat fires in central Kalimantan, Indonesia during the 2015 El Niño, *Atmos. Chem. Phys. Discuss.*, *1–37*, doi:10.5194/acp-2016-411.
- Van Damme, M., L. Clarisse, C. L. Heald, D. Hurtmans, Y. Ngadi, C. Clerbaux, A. J. Dolman, J. W. Erisman, and P. F. Coheur (2014), Global distributions, time series and error characterization of atmospheric ammonia (NH<sub>3</sub>) from IASI satellite observations, *Atmos. Chem. Phys.*, *14*(6), 2905–2922, doi:10.5194/acp-14-2905-2014.
- van der Werf, G. R., J. T. Randerson, L. Giglio, G. J. Collatz, M. Mu, P. Kasibhatla, D. C. Morton, R. DeFries, Y. Jin, and T. T. van Leeuwen (2010), Global fire emissions and the contribution of deforestation, savanna, forest, agricultural, and peat fires (1997–2009), *Atmos. Chem. Phys.*, *10*(23), 11,707–11,735, doi:10.5194/acp-10-11707-2010.



- Whitburn, S., M. Van Damme, J. Kaiser, G. van der Werf, S. Turquety, D. Hurtmans, L. Clarisse, C. Clerbaux, and P-F. Coheur (2015), Ammonia emissions in tropical biomass burning regions: Comparison between satellite-derived emissions and bottom-up fire inventories, *Atmos. Environ.*, *121*, 42–54, doi:10.1016/j.atmosenv.2015.03.015.
- Whitburn, S., M. Van Damme, L. Clarisse, S. Bauduin, C. Heald, J. Hadji-Lazaro, D. Hurtmans, M. Zondlo, C. Clerbaux, and P-F. Coheur (2016), A flexible and robust neural network IASI-NH<sub>3</sub> retrieval algorithm, *J. Geophys. Res. Atmos.*, *121*, 6581–6599, doi:10.1002/2016JD024828.
- Yurganov, L. N., et al. (2011), Satellite- and ground-based CO total column observations over 2010 Russian fires: Accuracy of top-down estimates based on thermal IR satellite data, *Atmos. Chem. Phys.*, *11*(15), 7925–7942, doi:10.5194/acp-11-7925-2011.